Volume 11
Number 10
14 March 2020
Pages 2575–2864

Chemical Science

rsc.li/chemical-science

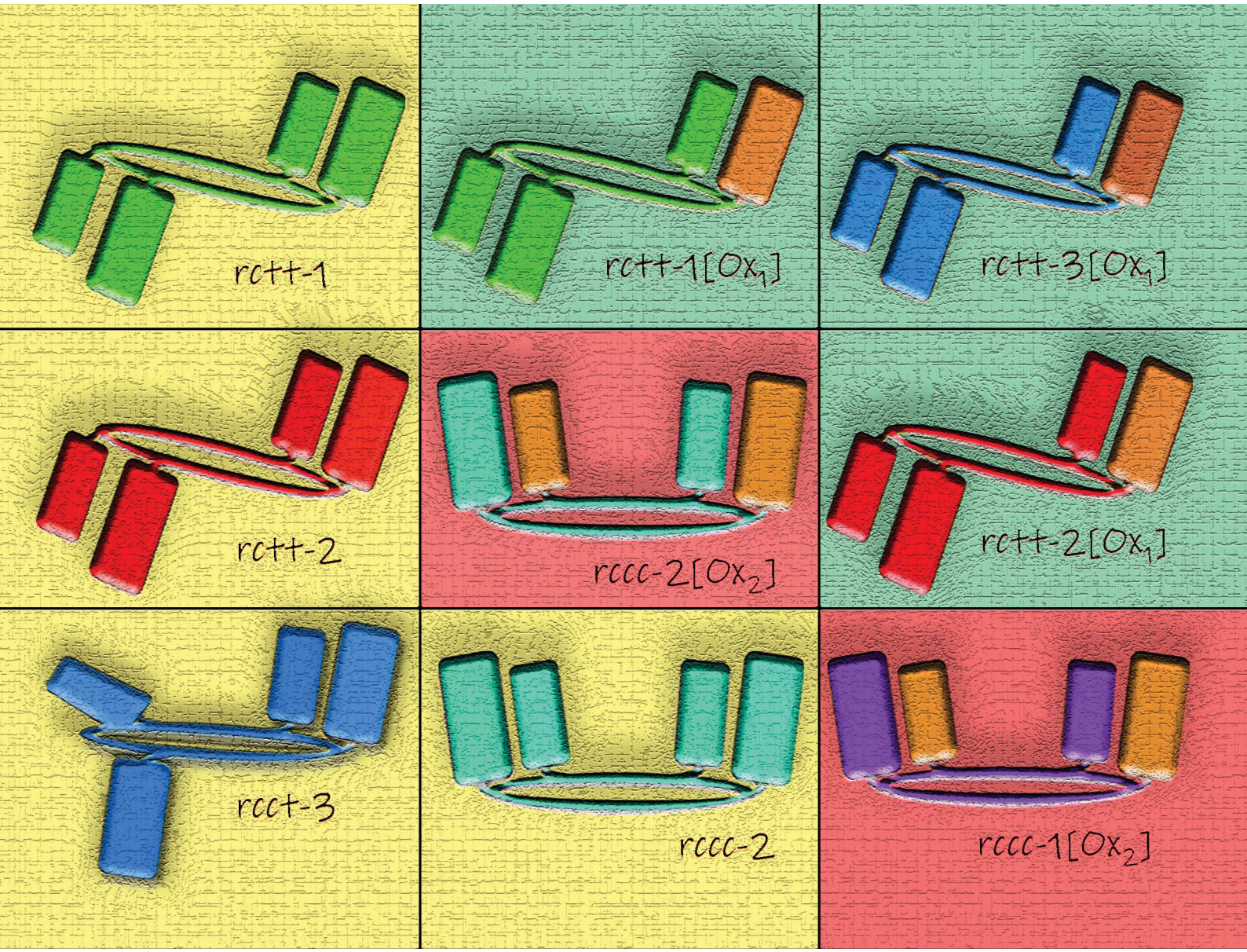

ISSN 2041-6539

ROYAL SOCIETY OF CHEMISTRY

EDGE ARTICLE

Francis D'Souza, Jonathan P. Hill *et al.*

Nanomolecular singlet oxygen photosensitizers based on hemiquinonoid-resorcinarenes, the fuchsonarenes

Chemical Science

ROYAL SOCIETY OF CHEMISTRY

EDGE ARTICLE

View Article Online
View Journal | View Issue

Cite this: *Chem. Sci.*, 2020, **11**, 2614

All publication charges for this article have been paid for by the Royal Society of Chemistry

Nanomolecular singlet oxygen photosensitizers based on hemiquinonoid-resorcinarenes, the fuchsonarenes†

Daniel T. Payne, [a] Whitney A. Webre,[b] Habtom B. Gobeze,[b] Sairaman Seetharaman,[b] Yoshitaka Matsushita, [c] Paul A. Karr,[d] Mandeep K. Chahal, [a] Jan Labuta, [a] Wipakorn Jevasuwan,[a] Naoki Fukata, [a] John S. Fossey, [e] Katsuhiko Ariga, [af] Francis D'Souza *[b] and Jonathan P. Hill *[a]

Received 4th February 2020
Accepted 11th February 2020

DOI: 10.1039/d0sc00651c

rsc.li/chemical-science

Singlet oxygen sensitization involving a class of hemiquinonoid-substituted resorcinarenes prepared from the corresponding 3,5-di-*t*-butyl-4-hydroxyphenyl-substituted resorcinarenes is reported. Based on variation in the molecular structures, quantum yields comparable with that of the well-known photosensitizing compound *meso*-tetraphenylporphyrin were obtained for the octabenzyloxy-substituted double hemiquinonoid resorcinarene reported herein. The following classes of compounds were studied: benzyloxy-substituted resorcinarenes, acetyloxy-substituted resorcinarenes and acetyloxy-substituted pyrogallarenes. Single crystal X-ray crystallographic analyses revealed structural variations in the compounds with conformation (*i.e.*, rctt, rccc, rcct) having some influence on the identity of hemiquinonoid product available. Multiplicity of hemiquinonoid group affects singlet oxygen quantum yield with those doubly substituted being more active than those containing a single hemiquinone. Compounds reported here lacking hemiquinonoid groups are inactive as photosensitizers. The term 'fuchsonarene' (fuchson + arene of resorcinarene) is proposed for use to classify the compounds.

Introduction

Several classes of chromophore are known to be capable of photosensitizing molecular oxygen through an energetic mechanism involving interaction of triplet excited state(s) of the chromophore with dioxygen,[1,2] which itself exists as a triplet ground state.[3] This process results in the generation of a singlet excited state of dioxygen, $^1O_2$, commonly referred to as singlet oxygen (SO), a highly reactive species widely considered as being detrimental when formed in the vicinity of, for instance, biological macromolecules such as nucleic acids or proteins.[4,5] Damage to these materials caused by singlet oxygen can ultimately lead to cell aging and carcinogenesis.[6] However, the destructive potential that makes SO hazardous can also be harnessed in beneficial applications. These applications are largely destructive involving photoinduced deactivation of undesirable biological entities[7,8] (*i.e.*, viruses, bacteria) and photodecomposition of environmental pollutants.[9,10] However, SO has also been used in a constructive sense, it being a highly effective reagent in chemical syntheses.[11,12] Photosensitized generation of SO underpins photodynamic therapy (PDT) where SO is generated in order to kill cancer cells. A therapeutic chromophore is administered depending on the disease condition followed by local irradiation at the disease site with an appropriate wavelength resulting in a high local concentration of SO. This reduces the viability of diseased cells or kills tumor tissues.[13,14] In research on macrocyclic systems, some porphyrins and metalloporphyrins, such as Temoporfin (tetrakis(3-hydroxyphenyl)chlorin) and Tookad (palladium bacteriopheophorbide),[15] have been approved for clinical use for cancer PDT[16,17] or to treat other conditions involving the elimination of abnormal cells (*e.g.*, macular degeneration[18]).

While porphyrins (*e.g.*, tetraphenylporphyrin, TPP[19]) and fluorone dyes (*e.g.*, Rose Bengal, RB[20]) are well known SO

[a]*International Center for Materials Nanoarchitectonics, National Institute for Materials Science, Namiki 1-1, Tsukuba, Ibaraki 305-0044, Japan. E-mail: Jonathan.Hill@nims.go.jp*

[b]*Department of Chemistry, University of North Texas, 1155 Union Circle, 305070 Denton, Texas 76203, USA. E-mail: francis.dsouza@unt.edu*

[c]*Research Network and Facility Services Division, National Institute for Materials Science (NIMS), 1-2-1 Sengen, Tsukuba, Ibaraki 305-0047, Japan*

[d]*Department of Physical Sciences and Mathematics, Wayne State College, 111 Main Street, Wayne, Nebraska 68787, USA*

[e]*School of Chemistry, University of Birmingham, Edgbaston, Birmingham, West Midlands, B15 2TT, UK*

[f]*Department of Advanced Materials Science, Graduate School of Frontier Sciences, The University of Tokyo, 5-1-5 Kashiwanoha, Kashiwa, Chiba 277-8561, Japan*

† Electronic supplementary information (ESI) available. CCDC 1934744–1934750. For ESI and crystallographic data in CIF or other electronic format see DOI: 10.1039/d0sc00651c

photosensitizers,[21] they suffer from several disadvantages such as aggregation or deactivation *in vivo* so that there remains a requirement to identify other effective chromophores to better understand structure–activity relationships of the compounds and to extend the application potential of the method. Therefore, in order to meet this demand, the SO photosensitizing properties of hemiquinone-substituted resorcinarenes have been studied and are reported here.[22] These resorcinarenes represent a potentially important class of photosensitizers due to their ease of functionalization, variable geometries and nanometric dimensions, all of which might be used to tune the applicable properties of the compounds.

Results

Design and synthesis

A new class of SO photosensitizers based on resorcinarenes,[23,24] which have not been previously investigated for this purpose, is reported. Whilst characterizing the optical properties of antioxidant-substituted resorcinarenes[22] (Fig. 1) in an earlier report, it was observed that the oxidized states of those molecules are capable of generating SO at levels to make them of interest in the aforementioned applications. Resorcinarene macrocycles present several advantages over other classes of compound in that they can be prepared in large quantities with high purity and are amenable to a wide range of chemical synthetic modifications. Furthermore, the relative disposition of substituents can be systematically varied by controlling macrocyclic conformation, *i.e.*, chair (rctt), crown (rccc), saddle (rcrc), *etc.*[25] For instance, the chair isomer rctt might be easily multiply substituted with large hydrophilic substituents providing water soluble globular molecules suitable for *in vivo* applications. Therefore, we have attempted in this work to establish the structure–property relationship between the substitution patterns of resorcinarenes (and also pyrogallarenes[26]) and their relative efficacies as SO photosensitizers. Chemical structures of the compounds are shown in Fig. 1. Molecules **1** have been reported previously[22] while **2**, **3** and **4** were additionally prepared to investigate the photosensitizing activity structure–property relationship. Resorcinarene and pyrogallarene compounds are tetrameric macrocycles respectively containing four 1,3-catechol or 1,2,3-trihydroxybenzene groups linked through four '*meso*' positions (pink circles in Fig. 1) formed by condensation with aldehydes. Any further functionality of the aldehyde is then incorporated at the macrocyclic *meso* positions. Here we have introduced antioxidant phenol groups as *meso*-substituents, which can be converted between different oxidation states: phenol or hemiquinonoid. The compounds can then be categorized as those not containing hemiquinonoid groups, those containing a single hemiquinonoid group (rctt-[Ox_1]-type), and those containing two hemiquinonoid groups (rccc-[Ox_2]-type). Molecular conformations of the molecules were detected using X-ray crystallography (described later) and the selection of conformer is largely due to the synthetic method. That is, [Ox_1]-type conformers are exclusively rctt, while [Ox_2]-type are obtained either by conformational switching of rctt to rccc or by oxidation of a precursor with the same conformation. Thus, rccc-**1**[Ox_2] is obtained from rctt-**1**[Ox_1] but rccc-**2**[Ox_2] can only be obtained by oxidation of rccc-**2** since rctt-**2**[Ox_1] resists oxidation. This feature is related to the oxidation potentials of the different compounds. A graphical representation of the

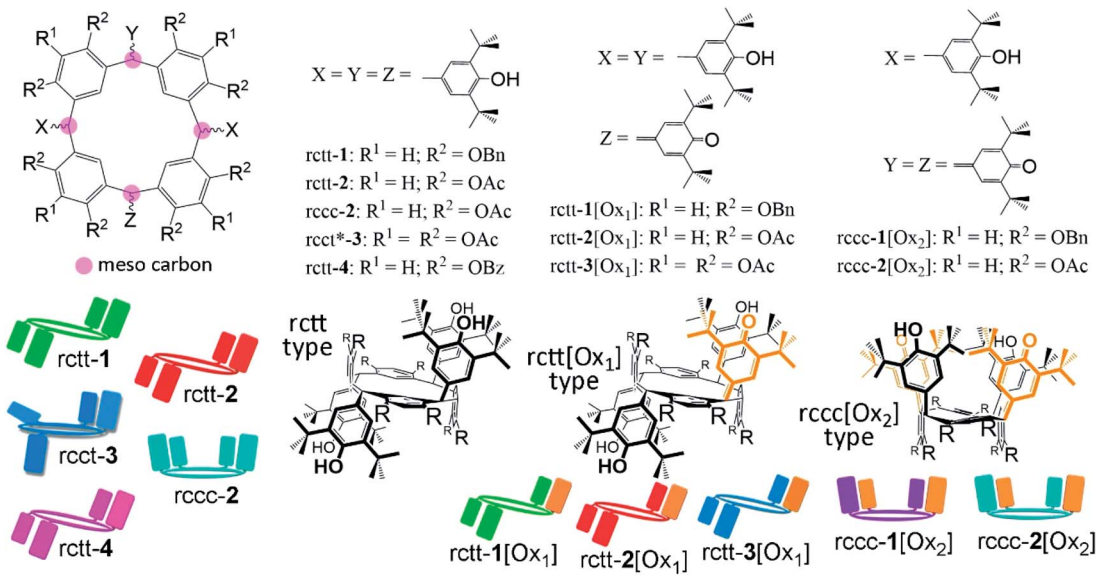

Fig. 1 Chemical structures of the compounds used in this report. Conformations of the molecules are denoted according to the key at bottom left and were found using single crystal X-ray structure determination. Representative chemical drawings of the corresponding conformers are also shown. The compounds are grouped according to their states of oxidation: [Ox_1] indicates a single *meso*-hemiquinonoid group; [Ox_2] indicates two *meso*-hemiquinononoid groups. The schematic representations of these compounds are colour-coded according to macrocyclic and substituent identity (green/purple: resorcinarene benzyl; red/turquoise: resorcinarene, acetate; blue: pyrogallarene, acetate) and rectangular substituent identity (same as ring: phenol; orange: hemiquinonoid).

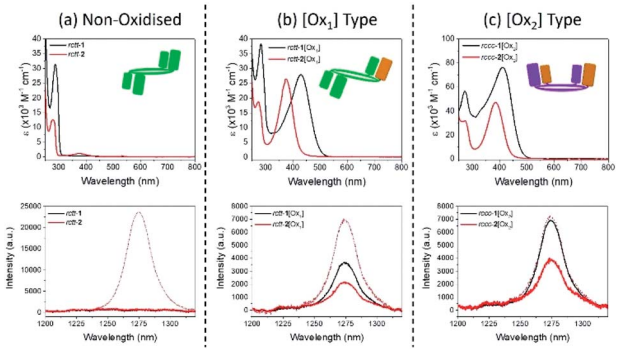

Fig. 2 Electronic absorption and singlet oxygen phosphorescence spectra for series **1** and **2** compounds at 6.10×10^{-5} mol dm^{-3} in chloroform: (a) non-oxidized: rctt-**1** (black) and rctt-**2** (red); (b) [Ox_1]-type: rctt-**1**[Ox_1] (black) and rctt-**2**[Ox_1] (red); (c) [Ox_2]-type: rccc-**1**[Ox_2] (black) and rccc-**2**[Ox_2] (red). Corresponding singlet oxygen emission spectra for series **1** and **2** compounds recorded in chloroform, with *meso*-tetraphenylporphyrin (TPP) reference responses shown as dotted lines (see ESI† for details).

compounds constructed based on chemical structure, conformation and oxidation state is also defined in Fig. 1 and used throughout this paper. Compounds **1**, **2** and **4** were obtained from the same resorcinarene precursor (Precursor A in the ESI†) while compounds **3** were obtained from the corresponding pyrogallarene precursor (Precursor B in the ESI†).

Singlet oxygen photosensitization

Singlet oxygen photosensitization by the compounds was investigated by studying the intensity of singlet oxygen phosphorescence emission at 1272 nm during irradiation of the compounds at their long wavelength absorbance maxima around 380 nm (generation of singlet oxygen under irradiation is also supported by electron spin resonance (ESR) in the presence of TEMP spin trap, and by endoperoxide formation of anthracene with monitoring by UV/Vis spectroscopy; see Fig. S8 and S9 in the ESI†). Fig. 2(a–c) shows the electronic absorption spectra of the benzylated compounds **1** (data for other compounds are shown in the ESI, Fig. S10†), and also the phosphorescence emission spectra in the infrared region. These spectra reveal the presence of singlet oxygen generated during irradiation of the compounds due to the appearance of the highly characteristic fluorescence emission peak of SO at 1272 nm.[27] Fig. 2(a) shows that rctt-**1** is not active as a photosensitizer and does not produce singlet oxygen during irradiation at 286 nm (although it is known that another reactive oxygen species, probably superoxide, is formed by similar irradiation of this compound[22]). In fact, all compounds lacking hemiquinonoid groups also lack SO photosensitizer activity (see ESI†). Fig. 2(b and c) indicate that singlet oxygen is generated by irradiation of rctt-[Ox_1]-type and rccc-[Ox_2]-type compounds at their long wavelength absorption maxima (see also Table 1). Irradiation at the short wavelength maxima around 286 nm gave no response from any of the compounds (see ESI, Fig. S11†).

Quantum yields of SO generation were estimated from the intensities of the SO fluorescence emission band at 1272 nm for each compound relative to that of *meso*-tetraphenylporphyrin (TPP, QY = 0.55 (ref. 28 and 29)) and are shown in Table 1. These data indicate that, of the compounds studied here, **1**[Ox_n] ($n = 1$, 2) are the most effective SO photosensitizers and that [Ox_2] states are optimum. Of the compounds studied, rccc-**1**[Ox_2] has the largest singlet oxygen quantum yield with $\Phi_{so} = 0.53$ making it a potentially useful new type of photosensitizer for SO generation. Acetates **2** and **3** exhibited comparatively moderate activity while compounds derived from oxidation of **4** could not be isolated.

Table 1 Estimated quantum yields of antioxidant-substituted resorcinarenes and pyrogallarenes used in this work. Sample solutions were excited at their respective absorption maxima

Entry	Compound	Excitation wavelength (nm)	Quantum yield (Φ_{so})
1 (ref. 28 and 29)	TPP	419	0.55
2	rctt-**1**	286	0
3	rctt-**2**	279	0
4	rccc-**2**	277	0
5	rcct*-**3**	276	0
6	rctt-**4**	275	0
7	rctt-**1**[Ox_1]	431	0.29
8	rctt-**2**[Ox_1]	377	0.17
9	rctt-**3**[Ox_1]	371	0.14
10	rccc-**1**[Ox_2]	412	0.53
11	rccc-**2**[Ox_2]	386	0.29

Chemical structural and electronic properties of the molecules should be considered to rationalize the optimization of photosensitizing activity in these compounds. X-Ray crystal structures of the compounds are shown in Fig. 3 together with graphical representations of the compounds which present their conformation and oxidation state of the substituents as depicted in Fig. 1. Compounds containing hemiquinonoid groups were prepared by treating the corresponding starting non-oxidized compounds with appropriate quantities of 2,3-dichloro-5,6-dicyano-1,4-benzoquinone (DDQ) followed by purification using column chromatography (see ESI†). In the **1** series of compounds, stepwise oxidation yields rctt-**1**[Ox_1] then rccc-**1**[Ox_2]. For the **2** series, rctt-**2** and rccc-**2** isomers can be isolated by the acetylation/fractional crystallization of a mixture of rctt and rccc isomers of their direct precursor (Precursor A – see ESI, Fig. S12†). rctt-**2** can also be prepared from the rctt-only isomer of its precursor according to a modified procedure (see ESI†). rctt-**2** and rccc-**2** were subsequently individually oxidized yielding respectively rctt-**2**[Ox_1] and rccc-**2**[Ox_2]. Notably, neither rctt-**2**[Ox_2] nor rccc-**2**[Ox_1] could be detected suggesting that the isomer identity affects oxidation state stability in **2** acetates (see Fig. S13†). Also, note that rctt-**2**[Ox_1] could not be directly converted to rccc-**2**[Ox_2] by treatment with DDQ despite this process being possible in the **1** series, leading to the requirement for method development to access the non-oxidized rccc macrocycle. Pyrogallarenes **3** are unusual in that rcct*-**3** is obtained from acetylation of the precursor (Precursor 'B' – see ESI†) while another unidentified isomer was neglected. The rcct* designation is based on the configuration of its *meso* protons (*meso* positions are indicated in Fig. 1 using pink circles) since one of the *meso*-phenyl substituents is somewhat distorted (*meso*-position is inverted) from the

expected form (denoted by *) being deflected towards the plane of the macrocycle (see Fig. 3). Interestingly, rctt-**3**[Ox_1] is generated by treatment with DDQ suggesting that the distorted substituent undergoes oxidation to the hemiquinonoid unit leading to the rctt isomer whereas oxidation of other substituents would maintain the rcct* conformation. [Ox_2]-type compounds could not be accessed in the **3** series. The benzoyl analogue of rctt-**2**, rctt-**4** was also prepared but any oxidized states formed by treatment with DDQ could not be isolated due to their instability during column chromatography.

The generally accepted mechanism of singlet oxygen formation during oxygen quenching of $\pi\pi^*$ triplet states involves the successive formation of an excited non-charge transfer encounter complex and a partial charge transfer exciplex of singlet and triplet multiplicities followed by interaction of triplet ground state with the triplet excited sensitizer.[30] In order to confirm formation of the triplet state and its oxygen quenching, transient absorption spectral studies were performed on representative rctt-**1** and rctt-**1**[Ox_1] in nitrogen-saturated and dioxygen-saturated solutions (for rctt-**1**[Ox_1] see Fig. 4). As expected no signal could be detected for rctt-**1** (which generates no SO) while for rctt-**1**[Ox_1] a band was found at 520 nm (excitation 355 nm in chloroform), as shown in Fig. 4. Although singlet oxygen generation is often observable on the nanosecond timescale,[31] in the case of rctt-**1**[Ox_1] a decaying absorbance band assigned to its triplet state could only be detected on a picosecond timescale (fs-TA, see Fig. 4). The decay of that signal could be fitted to a triexponential decay with lifetimes of 1323.5 (τ_1), 7.9 (τ_2) and 0.1 (τ_3) ps in a nitrogen atmosphere. The decay of this signal was considerably more rapid when the solution was purged with dioxygen (43.4 (τ_1), 8.5 (τ_2) and 1.4 (τ_3) ps) indicating that the 520/510 nm band is likely due to either a singlet/triplet mix state or a pure triplet state species, formed by intersystem crossing (ISC), which then interacts with dioxygen. Triplet state quenching of SO photosensitizer usually involves simple monoexponential decay. Triexponential decay and the significantly increased rate of quenching suggests that the mechanism involving rctt-**1**[Ox_1] may involve other processes, as does the persistent small non-zero absorption following excitation. Furthermore, for rccc-**1**[Ox_2] almost no difference could be detected in the persistence of the triplet state absorption in N_2- or O_2-saturated solutions by fs-TA (see Fig. S14†), although SO is certainly generated by irradiation of this compound, as confirmed by ESR and UV/Vis measurements (Fig. S8 and S9†), with optimum quantum yield for rccc-**1**[Ox_2] among the compounds studied here based on the SO phosphorescence emission at 1272 nm (Fig. 2 and Table 1). These observations can be explained by the increasingly

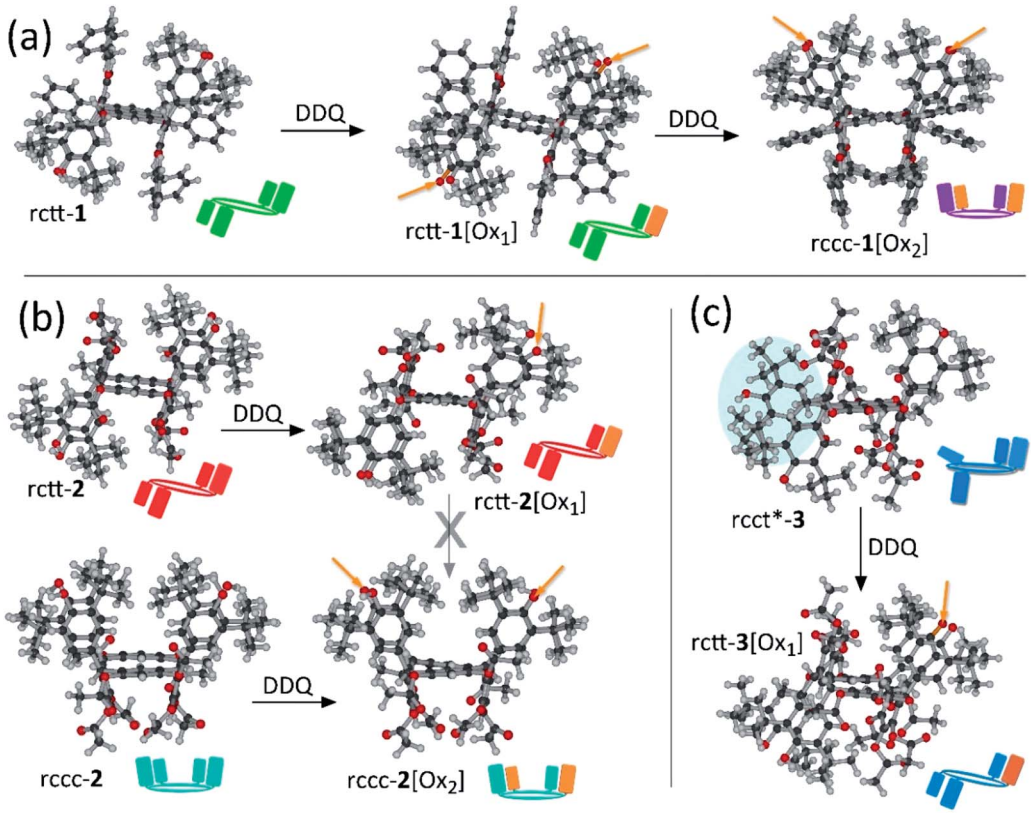

Fig. 3 X-Ray crystal structures of compounds **1**–**3**. (a) rctt-**1**, rctt-**1**[Ox_1] and rctt-**1**[Ox_2]. (b) rctt-**2** and rctt-**2**[Ox_1], rccc-**2** and rccc-**2**[Ox_2]. (c) rcct*-**3** and rctt-**3**[Ox_1]. For X-ray structure of **4** and other elevations of the compounds see ESI.† DDQ is 2,3-dichloro-5,6-dicyano-1,4-benzoquinone; arrow with cross denotes no oxidation detected under DDQ treatment. Carbonyl groups of [Ox_1] and [Ox_2] compounds are indicated by orange arrows. rctt-**1**[Ox_1] has its carbonyl group crystallographically disordered over two sites. [Ox_2]-type compounds crystallize with an rccc conformation. In rcct*-**3**, blue highlighting circle denotes the *meso*-substituent that is deflected towards the plane of the macrocycle associated with an inverted *meso*-position. Plan elevations of the molecules are shown in the ESI.†

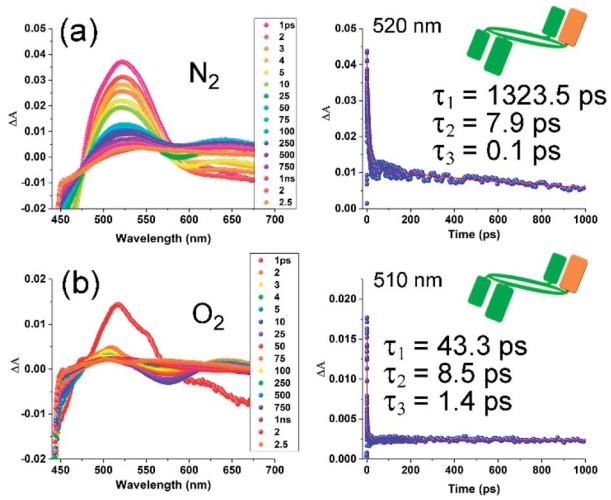

Fig. 4 Femtosecond transient absorption spectra at different delay times of rctt-**1**[Ox_1] in chloroform purged with (a) N_2 or (b) O_2. Traces at right show absorbance decay profiles at 520/510 nm for rctt-**1**[Ox_1] under N_2 and O_2.

rapid quenching of the triplet states of these compounds compared to other photosensitizers. That is, rctt-**1**[Ox_1] triplet quenching occurs on the femtosecond timescale while, we speculate, that of rccc-**1**[Ox_2] may be accelerated further so as not to be observable in the same regime. The reasons for the acceleration lie in the nanomolecular structures of the compounds, which introduce enhanced supramolecular interactions affecting energies of charge-transfer-assisted quenching and, in turn, rates of triplet state quenching.[32]

In the case of rctt-**1**[Ox_1], triexponential decay suggests other processes and this is, in fact, the case. ESR spectra obtained during irradiation of rctt-**1**[Ox_1] reveal the formation of phenoxyl radical signified by the characteristic spectrum.[33] This is due to the reaction of SO (generated by irradiation of rctt-**1**[Ox_1]) with antioxidant phenol groups of the photosensitizer. However, irradiation of rccc-**1**[Ox_2] does not yield any such radical species. This suggests that phenol groups adjacent to hemiquinone moieties either cannot form phenoxyl radicals or that, if formed, they are destabilized. For rctt-**1**[Ox_1], where two of the three available phenol groups are not proximal to a hemiquinone group, formation of phenoxyl radical is permitted, for rccc-**1**[Ox_2], both phenols are in the close vicinity of hemiquinones so that phenoxyl radical was not observed even under irradiation. That is despite temporal evolution of the ESR spectrum leading to the strongest intensity response of the TEMP/SO complex again supporting the observation that rccc-**1**[Ox_2] is the optimal SO generator of the compounds studied here. It has been reported that calixarene and resorcinarene macrocycles, and other molecules containing both quinone and hydroquinone or hemiquinone/phenol groups undergo intramolecular charge transfer (C-T) interactions.[22,34,35] Thus, we speculate that reduction in electron density on phenol groups caused by their proximity to electron deficient hemiquinones in the same molecule eliminates formation of phenoxyl radical in rccc-**1**[Ox_2] while two phenol groups of rctt-**1**[Ox_1] are sufficiently remote (see Fig. 3(a)) from its hemiquinone that reaction with singlet oxygen is permitted. Overall, the isomer structure and form of the compounds (*i.e.*, Ox_1 or Ox_2) controls their activity in relation to interactions with oxygen in turn affecting the efficiency of SO generation.

Discussion

As shown in the crystal structures of the compounds, the chromophore density in the compounds increases with oxidation state passing from [Ox_1]-type to [Ox_2]-type compounds and a corresponding increase in quantum yield of SO photosensitization. Also, macrocyclic 1,3-catechol substitution with benzyloxy groups is preferable to their esterification for optimization, which might be due to steric or electronic effects. Regardless of the reasons for differences in activities of the compounds, we were surprised to find photosensitizing activity at all for any of the compounds. However, in speculating on the chemical structures of the compounds there appears some correspondence with the structures of known photosensitizers, specifically fluorescein-type molecules such as Rose Bengal. Fig. 5 shows the chemical structures of the chromophore present in [Ox_n]-type compounds next to that of Rose Bengal, a well-documented SO photosensitizer.[20] A common feature of the molecules is a hemiquinonoid functionality conjugated with relatively electron rich phenyl groups similar to other fluorone-type dyes, although the forms of the compounds are, of course, quite different.

Molecular orbital structures of these compounds were investigated in order to understand the inter-component electronic interactions of the compounds. We performed DFT calculations using the X-ray crystallographic coordinates as starting points for the geometry optimizations. The structures of the frontier (HOMO and LUMO) molecular orbitals (in plan and side elevations) for groups of compounds **1**, **2** and **4** are shown in Fig. 6 (data for **3** are shown in the ESI†). For rctt-**1**, there is a wide HOMO–LUMO gap of 4.72 eV with the HOMO located on the macrocyclic portion of the molecule (*i.e.*, the resorcinarene) and LUMO distributed on two of its benzyl substituents. The HOMO of rctt-**1** is distributed over the resorcinarene macrocycle with small conjugative contributions from the *meso*-phenol substituents. For rctt-**1**[Ox_1], containing a single hemiquinonoid group, its HOMO is distributed over the conjugated quinonoid structure introduced by incorporation of the unsaturated *meso*-position, as

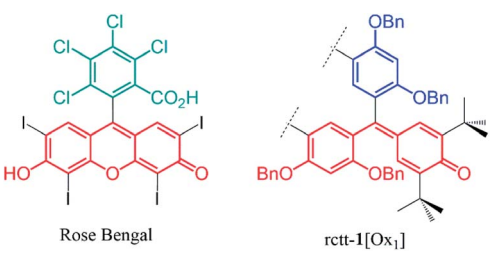

Fig. 5 Chemical structures of Rose Bengal (left) and the chromophore moiety of the structure of rctt-**1**[Ox_1] reveals a similar hemiquinonoid conjugated with electron rich aromatic substituents in the chromophore structure.

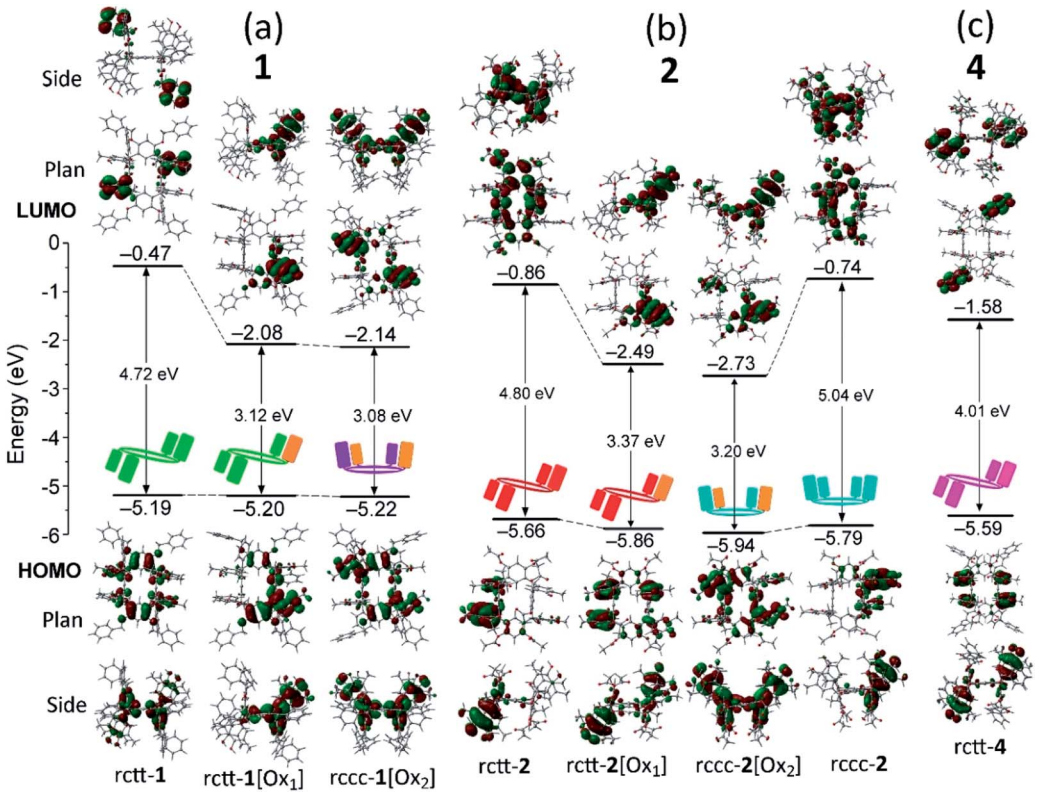

Fig. 6 Evolution of structure and energy levels of frontier molecular orbitals for (a) rctt-**1**, rctt-**1**[Ox_1] and rccc-**1**[Ox_2], (b) rctt-**2**, rctt-**2**[Ox_1], rccc-**2**[Ox_2] and rccc-**2**, and (c) rctt-**4**. Each frontier orbital is shown in plan and side elevation.

suggested by a structural comparison with fluorescein and other fluorone dyes (see Fig. 5). The LUMO level of rctt-**1**[Ox_1] is also stabilized by 1.61 eV over rctt-**1** due to the addition of the electron-withdrawing hemiquinone group. Introduction of a further hemiquinonoid group in rccc-**1**[Ox_2] leads to only minor variations in energy compared to rctt-**1**[Ox_1] also regardless of the change in isomer structure. This is consistent with the electronic absorption spectroscopy of these compounds where the long wavelength absorption maxima at 380 nm only increases in intensity with a minor reduction in energy of the peak (see Fig. 2). The HOMO structure of rccc-**1**[Ox_2] (see Fig. 6) contains two highly conjugated chromophore units similar to that in rctt-**1**[Ox_1] but the only minor differences in energy level and electronic absorption spectra between rccc-**1**[Ox_2] and rctt-**1**[Ox_1] indicate that these are not themselves inter-conjugated so that the improved SO generating properties of rccc-**1**[Ox_2] appear due simply to doubling of the concentration of the SO chromophore.

Corresponding trends can be observed for the molecular orbital structures of compounds **2** and **3** with HOMOs largely distributed on the macrocycle and LUMOs residing on hemiquinonoid groups conjugated with the directly bonded catechol moieties of the macrocycle (see Fig. 6 and S15 in the ESI,† resp.). Similar reductions in the energy of the LUMO orbital were found on the respective oxidations of rctt-**2** or rccc-**2** to rctt-**2**[Ox_1] and rccc-**2**[Ox_2], associated with similar changes in the HOMO–LUMO energy gap. Compound rctt-**4** behaves similarly to rctt-**1** in that its frontier LUMO is located on two benzoyl substituents.

Conclusions

The oxidation of antioxidant-substituted resorcinarene (and pyrogallarene) macrocycles yields hemiquinonoid-substituted resorcinarenes (and pyrogallarene), which act as singlet oxygen photosensitizers. Variations in the chemical structure and conformation of the macrocycles establish that the optimal resorcinarene molecular structure for SO photosensitization (of the compounds studied here) contains two hemiquinonoid *meso*-substituents with benzyloxy groups at macrocyclic catechol substituent positions. Quantum yields of singlet oxygen generation for the optimal compound rccc-**1**[Ox_2] reach levels similar to the well-known SO photosensitizer *meso*-tetraphenylporphyrin. This work opens up a new avenue for research on the potential applications of the nanomolecular resorcinarene macrocycles and their properties. Also, by analogy with the fuchsone dyes, whose structures these resorcinarenes resemble, we propose the portmanteau term 'fuchsonarenes' for the classification of these compounds since they exhibit structural and chemical properties of both classes of molecules.

Author contributions

D. T. P. and J. P. H. designed the experiments, performed synthesis and chemical analyses of the compounds, W. A. W.

performed singlet oxygen generation analyses and electrochemistry, H. B. G. and S. S. performed the transient absorption studies, Y. M. performed X-ray crystallography, P. A. K. undertook computational work, M. K. C. performed synthetic procedures, J. L. and J. S. F. analysed chemical analytical data, W. J. and N. F. collected electron spin resonance data, J. S. F, K. A. and F. D. undertook discussions of the experimental design and data. D. T. P. and J. P. H. composed and wrote the manuscript with scientific discussions and contributions from all co-authors.

Conflicts of interest

There are no conflicts to declare.

Acknowledgements

This work was partly supported by World Premier International Research Center Initiative (WPI Initiative), MEXT, Japan. The authors are grateful to Japan Society for the Promotion of Science (JSPS) for a JSPS Fellowship (to D. T. P.). This work was also partially supported by JSPS KAKENHI (Coordination Asymmetry) (Grant No. JP16H06518), and CREST, JST (Grant No. JPMJCR1665). This work was partly financially supported by the National Science Foundation (Grant No. 1401188 to FD). DFT calculations were carried out at the Holland Computing Center of the University of Nebraska.

References

1 O. J. Stacey and S. J. A. Pope, *RSC Adv.*, 2013, **3**, 25550–25564.
2 R. W. Redmond and J. N. Gamlin, *Photochem. Photobiol.*, 1999, **70**, 391–475.
3 W. T. Borden, R. Hoffmann, T. Stuyver and B. Chen, *J. Am. Chem. Soc.*, 2017, **139**, 9010–9018.
4 J.-L. Ravanat, P. Di Mascio, G. R. Martinez, M. H. G. Medeiros and J. Cadet, *J. Biol. Chem.*, 2000, **275**, 40601–40604.
5 M. J. Davies, *Biochem. Biophys. Res. Commun.*, 2003, **305**, 761–770.
6 L. F. Agnez-Lima, J. T. A. Melo, A. E. Silva, A. H. S. Oliveira, A. R. S. Timoteo, K. M. Lima-Bessa, G. R. Martinez, M. H. G. Medeiros, P. Di Mascio, R. S. Galhardo and C. F. M. Menck, *Mutat. Res., Rev. Mutat. Res.*, 2012, **751**, 15–28.
7 D. Garcia-Fresnadillo, *ChemPhotoChem*, 2018, **2**, 512–534.
8 P. Di Mascio, G. R. Martinez, S. Miyamoto, G. E. Ronstein, M. H. G. Medeiros and J. Cadet, *Chem. Rev.*, 2019, **119**, 2043–2086.
9 J. P. Escalada, A. Pajares, J. Gianotti, A. Biasutti, S. Criado, P. Molina, W. Massad, F. Amat-Guerri and N. A. García, *J. Hazard. Mater.*, 2011, **186**, 466–472.
10 R. Martinez-Haya, M. A. Miranda and M. L. Marin, *Catal. Today*, 2018, **313**, 161–166.
11 A. A. Ghogare and A. Greer, *Chem. Rev.*, 2016, **116**, 9994–10034.
12 A. Sagadevan, K. C. Hwang and M.-D. Su, *Nat. Commun.*, 2017, **8**, 1812.
13 F. Anquez, I. El Yazidi Belkoura, P. Suret, S. Randoux and E. Courtade, *Laser Phys.*, 2013, **23**, 025601.
14 L. C. B. Ramos, M. S. P. Marchesi, D. Callejon, M. D. Baruffi, C. N. Lunardi, L. D. Slep, L. M. Bendhack and R. S. da Silva, *Eur. J. Inorg. Chem.*, 2016, 3592–3597.
15 R. Baskaran, J. Lee and S.-G. Yang, *Biomater. Res.*, 2018, **22**, 25.
16 S. B. Brown, E. A. Brown and I. Walker, *Lancet Oncol.*, 2004, **5**, 497–508.
17 M. C. DeRosa and R. J. Crutchley, *Coord. Chem. Rev.*, 2002, **233–234**, 351–371.
18 R. Aquaron, J.-L. Murati, G. Fayet, C. Aquaron and B. Ridings, *Cell. Mol. Biol.*, 2002, **48**, 925–930.
19 A. D. Adler, F. R. Longo, J. D. Finarelli, J. Goldmacher, J. Assour and L. Korsakoff, *J. Org. Chem.*, 1967, **32**, 476.
20 J. J. M. Lamberts and D. C. Neckers, *Z. Naturforsch., B: Anorg. Chem., Org. Chem.*, 1984, **39**, 474–484.
21 H. Abrahamse and M. R. Hamblin, *Biochem. J.*, 2016, **473**, 347–364.
22 D. T. Payne, W. A. Webre, Y. Matsushita, N. Zhu, Z. Futera, J. Labuta, W. Jevasuwan, N. Fukata, J. S. Fossey, F. D'Souza, K. Ariga, W. Schmitt and J. P. Hill, *Nat. Commun.*, 2019, **10**, 1007.
23 C. M. A. Gangemi, A. Pappalardo and G. T. Sfrazzetto, *Curr. Org. Chem.*, 2015, **19**, 2281–2308.
24 P. Timmerman, W. Verboom and D. N. Reinhoudt, *Tetrahedron*, 1996, **52**, 2663–2704.
25 R. S. Patil, C. Zhang and J. L. Attwood, *Chem.–Eur. J.*, 2016, **22**, 15202–15207.
26 A. Ahman, M. Luostarinen, C. Schalley, M. Nissinen and K. Rissanen, *Eur. J. Org. Chem.*, 2005, 2793–2801.
27 C. Schweitzer and R. Schmidt, *Chem. Rev.*, 2003, **103**, 1685–1757.
28 R. Schmidt, K. Seikel and H.-D. Brauer, *J. Phys. Chem.*, 1989, **93**, 4507–4511.
29 R. Schmidt and E. Afshari, *J. Phys. Chem.*, 1990, **94**, 4377–4378.
30 C. Schweitzer, Z. Mehrdad, A. Noll, E.-W. Grabner and R. Schmidt, *J. Phys. Chem. A*, 2003, **107**, 2192–2198.
31 For example see: L. Sobotta, P. Fita, W. Szczolko, M. Wrotynski, M. Wierzchowski, T. Goslinski and J. Mielcarek, *J. Photochem. Photobiol., A*, 2013, **269**, 9–16.
32 Z. Mehrdad, C. Schweitzer and R. Schmidt, *J. Phys. Chem. A*, 2002, **106**, 228–235.
33 The ESR spectrum is reminiscent of galvinoxyl radical based on similar substitution patterns and splitting with meta-H and the proton at the macrocyclic meso position. See: (*a*) L. Lampp, M. Azarkh, M. Drescher and P. Imming, *Tetrahedron*, 2019, **75**, 2737–2747; (*b*) J. M. Cho, C. E. Song, S.-J. Moon, W. S. Shin, S. Hong, S. H. Kim, S. Cho and J.-K. Lee, *Org. Electron.*, 2018, **55**, 21–25.
34 B. Kim, G. Storch, G. Banerjee, B. Q. Mercado, J. Castillo-Lora, G. W. Brudwig, J. M. Mayer and S. J. Miller, *J. Am. Chem. Soc.*, 2017, **139**, 15239–15244.
35 O. B. Youchret-Zallez, S. Besbes-Hentati, M. Bouvet and H. Said, *J. Inclusion Phenom. Macrocyclic Chem.*, 2014, **79**, 383–390.

